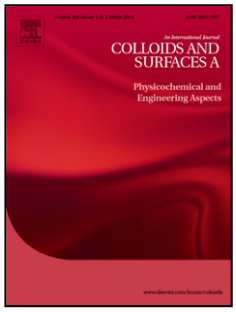

Title: Simple and novel strategies to achieve shape and size control of magnetite nanoparticles intended for biomedical applications

Author: Pamela Azcona Roberto Zysler Verónica Lassalle

PII: S0927-7757(16)30390-9
DOI: http://dx.doi.org/doi:10.1016/j.colsurfa.2016.05.064
Reference: COLSUA 20688

To appear in: *Colloids and Surfaces A: Physicochem. Eng. Aspects*

Received date: 29-3-2016
Revised date: 18-5-2016
Accepted date: 23-5-2016

Please cite this article as: Pamela Azcona, Roberto Zysler, Verónica Lassalle, Simple and novel strategies to achieve shape and size control of magnetite nanoparticles intended for biomedical applications, Colloids and Surfaces A: Physicochemical and Engineering Aspects http://dx.doi.org/10.1016/j.colsurfa.2016.05.064

Simple and novel strategies to achieve shape and size control of magnetite nanoparticles intended for biomedical applications

Pamela Azcona[1], Roberto Zysler[2] , Verónica Lassalle[1*]

[1]INQUISUR–UNS-CONICET, AvdaAlem 1253, 8000, B. Blanca, Bs As, Argentina
[2]Centro Atómico Bariloche—Instituto Balseiro, S. C. de Bariloche, RN, Argentina

[*]Corresponding author. E-mail addresses: veronica.lassalle@uns.edu.ar, (V.L. Lassalle). Tel. +54 0291 4595101 ext.3534,FAX +54-0291-4595187.

Graphical abstract

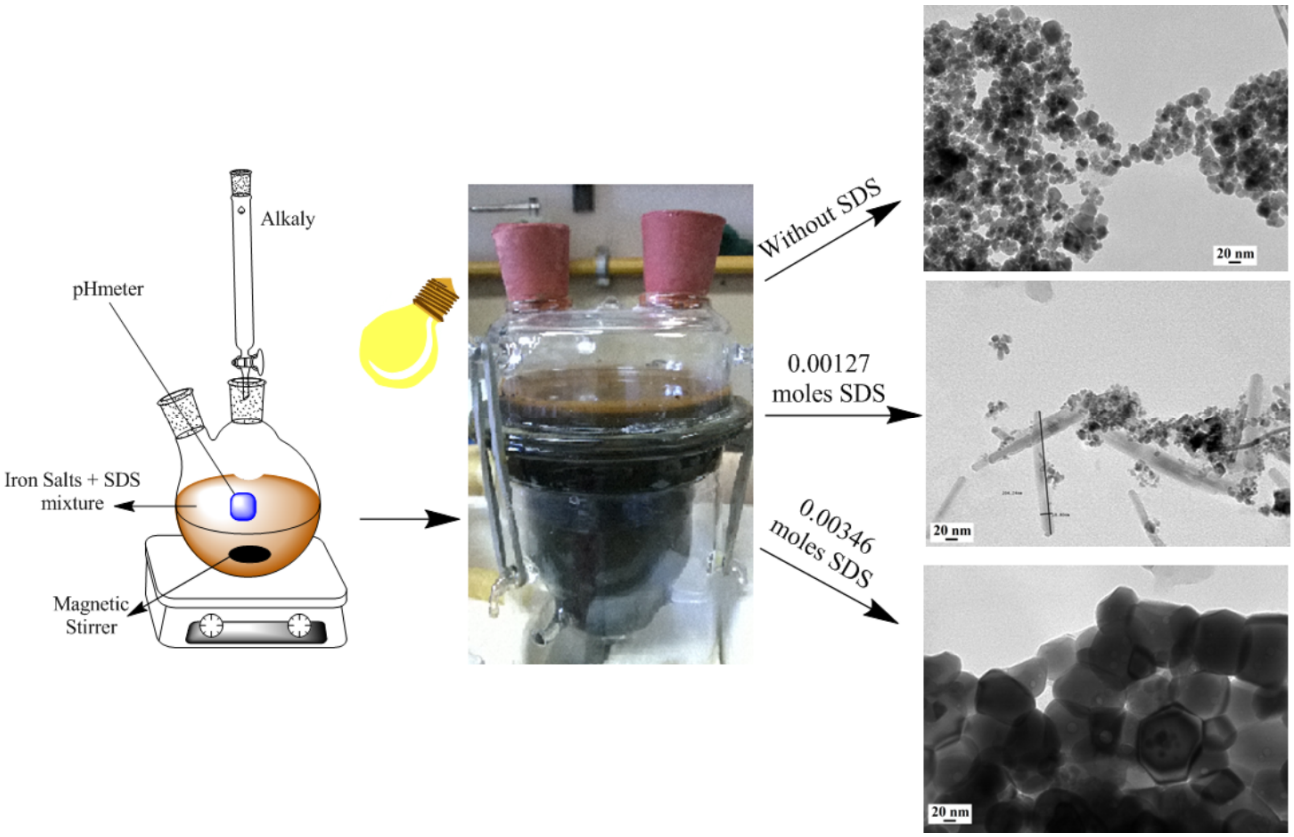

Highlight

- Magnetite based nanoparticles with specific size and shape.
- Simplification of traditional co-precipitation method.
- Role of sodium dodecyl sulfate on the shape of magnetite nanoparticles.
- Influence of other experimental parameters on MNPs properties.
- Stable and water-dispersible magnetic nanoparticles highly suitable for biomedical purposes.

ABSTRACT

Monodisperse magnetite nanoparticles (MNPs) with controlled sizes and shapes were prepared. The synthesis was carried out by traditional and inverted co-precipitation method with some modifications such as presence of visible light, room temperature and absence of inert atmosphere. Sodium dodecyl sulphate (SDS) was employed as stabilizer. The mentioned experimental parameters were conveniently adjusted to obtain suitable MNPs, to be efficiently employed in biomedical applications. In particular the size, shape, surface charge and magnetic properties were evaluated. MNPs were thoroughly characterized. From characterization data, it emerged that the inverted co-precipitation in presence of visible light rendered mainly nanorods. Modifying the SDS concentration the shape was tuned from nanorods to nanospheres and finally, at higher concentrations, nanocubes were obtained. All prepared formulations resulted hydrophilic. This property was justified in terms of the stabilization mechanism of SDS. Stability of MNPs aqueous dispersions was evaluated regarding to the variation of hydrodynamic diameter as a function of the time. In this regard, all the formulations resulted stable during, at least, 30 days. The prepared nanosystems exhibited satisfactory magnetic properties with saturation magnetization slightly lower than raw magnetite.

The combination of size, shape, surface charge, hidrophilicity and magnetic behaviour make the magnetic nanosystems here obtained highly suitable and promising to diagnostic and therapeutic applications.

Keywords: MAGNETIC NANOPARTICLES; CO-PRECIPITATION; MAGNETITE; IRON OXIDES; NUCLEATION AND GROWTH.

1. INTRODUCTION

It is well known that the interest in iron oxides nanoparticles investigation has grown radically during last decades regarding to the potential of these systems in several relevant fields such as medicine, environmental remediation and electronics [1,2].

In particular, magnetite (Fe_3O_4) in the nanosize has gained special interest due to its high magnetization and relatively low toxicity [3]. However, the control of size and morphology of these nanoparticles has become in a great challenge among researchers[4-6].This control would derive in nanoparticles with more specific properties that could be employed more efficiently in the mentioned, among other, areas [3]. For instance, different in vivo effects have been observed by employing spherical or needle shape MNPs [7, 8]. Similarly the surface charge of MNPs appears to be crucial regarding to the uptake capability at cellular level [9].

The preparation of uniform and almost individual MNPs may be achieved by using complex, expensive and energy consuming methods such as the acetyl acetanoate of Fe, the polyol , between others [10]; but it is particularly difficult when a simple, low cost and non time consuming method such as co-precipitation is intended. This well-known procedure includes aqueous iron salt (Fe^{2+}/Fe^{3+}) solutions; and a base as precipitant agent. The methodology is commonly performed under inert atmosphere at relatively high temperatures (70-90ºC) [10, 11]. The resulted particles generally exhibit a random morphology and size. Another limitation is associated to the aggregation trend in the co-precipitation media. Iron oxide particles tend to form large clusters due to the anisotropic dipolar attraction, and therefore mislay the particular properties related to single-domain magnetic nanostructures [10].

It is, therefore, of significant interest to increase the understanding of the underlying mechanism, looking for an acute control of the mentioned-among other- properties of MNPs. It has been extensively reported that slight variations of experimental conditions associated to co-precipitation may turn in near monodisperse nanoparticles with substantially different and well defined properties [12, 13]. Previous own works were devoted to reach MNPs with specific characteristics, that could be obtained by the precise control of experimental variables during co-precipitation. Some of those formulations were successfully used as carriers for the target of drugs [14-17].

Similar works are found in open literature; for instance, Roth *et al*. have explored the influence of a number of experimental variables (i.e: salt concentration, reaction temperature, ratio of hydroxide ions to

iron ions and ratio ofFe^{3+}/Fe^{2+}). They focused mainly in the impact of these variables in magnetization and in size. In this regards, they found that saturation magnetization may be improved by modifying Fe^{2+}/Fe^{3+} ratio and increasing the iron salts concentration. The particle size was affected by both iron salt concentration and also by the hydroxide ions to iron ions ratio [18].

Fang *et al.* evaluated the effect of temperature and base addition rate on the size of magnetite nanoparticles using co-precipitation process [19]. They found that rapid mixing directly affected the particle´s sizes. They also reported that temperature further influenced the sizes.

The effect of the kind of base was studied by Mascolo*et al*. These authors tested three different bases: NaOH, KOH or $(C_2H_5)_4NOH$ performing the co-precipitation at room temperature (r.t). They reported a relationship between the agglomeration trend of the nanoparticles and the pH developed in the co-precipitation media. Such pH strongly depended on the nature of the alkali [20].

The presence of additives such as surfactants was another variable highly studied. In a recent work, MNPs were synthesized by co-precipitation and modified with sodium dodecyl sulphate (SDS) in a post-synthesis step. These nanoparticles were used for the removal and recovery of copper, nickel and zinc from industrial wastewater. This article reported that high adsorption capacities may be obtained in a very short time (1 min) due to the very high surface area and short diffusion route of the SDS-coated Fe_3O_4 MNPs [21].

The present work is devoted to achieve a control of three relevant properties of magnetite nanoparticles: size, shape and surface charge. The goal is to obtain monodomain magnetic nanoparticles that may be tuneable by simply changing the experimental conditions associated to the preparation methodology. Co-precipitation was the selected method due to their versatility, and the advantages above mentioned. Among the vast information in open literature regarding to this method [18, 22, 23], a different focus is here provided. Since conditions such as presence of surfactant (using SDS), kind of alkali, rate of base addition, presence of visible light, order of reactants addition and the total volume of reaction mixture were analysed once a time fixing the rest of the variables.

To the best of these authors knowledge, the combination of the mentioned conditions has not been earlier explored in open literature. The work of Zhang *et. al* reports the preparation of magnetite (Fe_3O_4) nanorods using inverted co-precipitation at r.t and under the influence of an external magnetic field. However, they did not employ any stabilizer or additive during the synthesis [24].

Similarly Lin *et al.* used monowavelength light-emitting diode (LED) lamps irradiation at room temperature to prepare magnetite nanoparticles. Nevertheless, these authors did not employ co-precipitation. Instead, they obtained MNPs by aerial oxidation Fe II-EDTA solution [25].

In other works the shape of magnetite nanoparticles was altered by modifying reaction temperature and the base concentration by co-precipitation or the concentration of SDS [26, 27]. But, non-other experimental conditions were explored.

This contribution aims to further relating the mechanisms governing magnetite nanoparticles formation with their final properties and stability in view of their application in the biomedical field.

2. MATERIALS AND METHODS

2.1.-Materials

All reagents and solvents were of analytical grade and used without further purification. Ferric chloride hexahydrate (99.99%) and SDS were provided by Biopack (Argentina). Ferrous sulphate heptahydrate (99.99%) was provided by Mallinckradt Chemical Works (USA). Sodium hydroxide and Ammonium hydroxide solution (28-30%) were purchased from Cicarelli (Argentina). Absolute Ethanol was provided by Quimicor (Argentina). Destilled water with conductivity about 5.00 µS was employed.

2.2-Methods

2.2.1- Synthesis of magnetite by co-precipitation method.

Magnetite nanoparticles were synthesized by co-precipitation applying modifications with respect to the traditional methodology [15, 28]. Briefly, 5.4075g of $FeCl_3.6H_2O$ and 2.8g $FeSO_4.7H_2O$ (ratio Fe^{3+}/Fe^{2+}= 2/1)were dissolved in 100 ml of distilled water using a magnetic stirrer at room temperature and in absence of inert atmosphere. Different amounts (0– 1.0g) of SDS were added to this solution under stirring. The magnetite precipitation was achieved by raising the pH of the mixture to 12 by addition of different volumes of alkali. The alkali addition was performed at controlled rate to minimize aggregation. The described procedure was carried out in presence and absence of visible light generated by a tungsten lamp. The lamp was placed 10 cm from the reactor with a 90 degrees angle. Finally, the obtained dark solution was decanted using a magnet and the supernatant was extracted. The precipitate was washed several times with distilled water or a mixture ethanol/distilled water 50/50 solution. This procedure was

repeated until pH and conductivity reached the levels corresponding to distilled water. The solid was dried in oven at 45◦C overnight under vacuum.

The inverted co-precipitation was conducted by adding the Fe^{2+}/Fe^{3+} aqueous solution containing the proper amount of SDS to the alkali solution.

Table 1 includes the explored experimental conditions, whereas Scheme 1 depicted these synthetic routes.

2.2.2. Stability assays

The stability of MNPs was estimated in terms of the evolution of their size as a function of the time. To do this among 0.4mg and 1 mg of MNPs were placed in 10 mL of distilled water or in of a mixture ethanol/distilled water 50/50 depending on the MAG formulation. All samples were ultrasonicated during 60 min to measure the average hydrodynamic diameter. The measurements were performed once a week during 3 months.

2.3-Characterization Techniques

2.3.1-FTIR spectroscopy.

Transmission Infrared Fourier Transform Spectroscopy (FTIR) was performed using a Thermo Scientific Nicolet iS50 NIR module with Integrating Sphere in the frequency range 4000-400 cm-1. A few milligrams of the samples (10–20 mg) were mixed in a mortar manually with ~50 mg of KBr dry powder. The mixture was compacted and placed in the sample unit of the FTIR spectrometer.

2.3.2-Electron microscopy

Transmission electron microscopy (TEM, JEOL 100 CX II, Tokyo, Japan) were used to examine the morphology and estimate the size of the nanoparticles. The TEM samples were dispersed in distilled water or ethanol, placed on 200 mesh Cu grids and dried at room temperature.

2.3.3-Thermogravimetric analyses

Thermogravimetric analyses (TG) were performed using a Rigaku DTA-TAS 1000 equipment. Different masses of magnetic nanoparticles, magnetite and SDS were weighted and heated from room temperature to 500°C at a rate of 10°C/min under air atmosphere.

2.3.4-Hydrodinamic diameter and Z potential

A Malvern Zetasizer was used to measure the Z potential (ζ) and the hydrodynamic average particle diameter (HD, nm). Aqueous dispersions of MNPs were prepared at a concentration of 0.1 mg MNPs/ml

to measure the ζ. MNPs dispersed distilled water, to measure HD. In the last case the samples were ultrasonicated during 60 min previously to the assay. The informed values were an average of about five-seven repeated measurements.

2.3.5-Magnetic properties

Magnetic properties were measured using a commercial vibrating sample magnetometer (VSM) at room temperature with a magnetic field in the -10 to +10 kOe range. The sample was used as a powder, weighed and then placed in the sampler unit for measurement.

3.RESULTS AND DISCUSSION

The well-known traditional methodology to prepare magnetite by co-precipitation has been modified. Therefore, visible light, room temperature and air were implemented instead of inert atmosphere, and high temperature. The general mechanism associated to the iron oxides synthesis by this method is described by the following equations:

$$Fe^{3+} + 3OH^- \longrightarrow Fe(OH)_3 \quad (1)$$

$$Fe(OH)_3 \longrightarrow FeO(OH) + H_2O \quad (2)1)$$

$$Fe^{2+} + 2OH^- \longrightarrow Fe(OH)_2 \quad (3)$$

$$2FeO(OH) + Fe(OH)_2 \longrightarrow Fe_3O_4 + 2H_2O \quad (4)$$

Such mechanism is based on the nucleation of iron oxide particles and posterior growth. At the very early stages, the number and size of magnetic nucleus are very sensitive and to strongly dependent of the experimental conditions.

3.1.-Effect of the SDS incorporation and its concentration

The FTIR spectra of MAG-1, MAG-8 and MAG-7, are compared in Figure 1a, whereas Figure 1b shows the spectrum of pure SDS. It is worth mention that substoichiometric magnetite shows two bands at 586 and 404 cm^{-1}.Whereas maghemite spectrum exhibits peaks in the same region. Therefore, in MAG-7 spectrum, the typical Fe-O stretching band, observed at 570cm^{-1}, may be ascribed to magnetite as the predominant iron oxide.

Other signals observed in MAG 7 spectrum may be associated to both, CO_2 from air as well as residual water [29].

The peaks at 2900 cm^{-1}, that are due to the stretching vibration of C–H bonds in SDS (See Figure 1b), may be distinguish in MAG-1 and MAG-8 spectra, respectively. SDS typical peaks such as those located at ~1217 cm^{-1} and ~1086 cm^{-1}, associated to -S=O, are clearly observed in MAG-1 spectrum(See Figure 1a). These data give evidence that the kind of interaction established between iron oxide surface and the surfactant is dependent on SDS concentration [30]. It is worth noting that other signals typical of SDS , such as those at 3400-3450 cm^{-1} (ν OH) and 1650-1700 cm^{-1} (ν C-O)overlap with signals found in raw magnetite ascribed to CO_2 or surface adsorbed water molecules.

The ζ data included in Table 2, reveal that the surface charge of MAG did not change substantially by the incorporation of increasing nominal SDS concentrations.

XRD results ofMAG-1 and MAG-7 are shown in Figure 1c. From the Figure, it is clear that in both cases the positions of diffraction peaks match with those of Fe_3O_4 on comparison with the standard diffraction peaks of bulk iron oxides [31]. The peaks in MAG-7 diffractogram resulted narrower than the corresponding to MAG-1.

It is important to highlight that from the proposed synthetic path ways almost exclusively magnetite is obtained. Although the presence of maghemite is not easily verified (al least using the techniques employed within this work), it could be corroborated by UV visible spectroscopy. According to the work of Sutka et al great differences are observed analysing a dispersion of magnetite and maghemite NPs by UV visible spectroscopy. In fact they reported that the UV-vis absorption spectra of magnetite exhibits intense adsorption that remains constant (A=1.5) in all the explored UV visible range (400 to 1100nm).In the case of maghemite they showed an adsorption edge at ~780 nm, indicating an opening of the band gap [32].Hence, we have prepared an aqueous dispersion of MAG7 (0.17mg de MAG/mLof dispersion) and measured by UV –spectroscopy. The obtained spectrum is shown in the Figure f in Supplementary material. The profile observed fits well with the corresponding to magnetite NPs since non peaks or adsorption edges are observed in the region near 800nm.

The morphology and size (in terms of HD) was highly sensitive to the SDS concentration. Noticeable differences in shape and sizes were registered comparing TEM data arising from MAG-7, MAG-1 and MAG-8. Such differences are depicted in Figure 2 (see also Table 2). It is seen that raw magnetite nanoparticles are mainly spherical in shape and highly aggregated in water dispersion leading to an

average HD of about 400nm (see Figure 2a). The addition of SDS reduced the aggregation, leading to smaller particles (HD around 249nm) and roughly monodisperse. However, MAG-1 resulted greatly heterogeneous regarding to its shape. The addition of extra SDS (MAG-8) reduced aggregation of the particles. In fact, hydrodinamic diameters of MAG-8 fell to 198nm whereas the corresponding to MAG-1 was about 249 nm, both measured in identical conditions (see Table 2).

This behaviour enables us to assume that SDS binds preferentially specific lattices in the nucleus in formation. This fact restricts the growth of specific planes of MNPs and favours other planes. The ensuing consequence was the different shape in each case [33-35].

The preferential growth of specific planes in the magnetite lattice is associated to the surface energy of each plane. According to the literature the order would be: $\gamma\{1\ 1\ 1\} < \gamma\ \{1\ 0\ 0\} < \gamma\ \{1\ 1\ 0\}$ [36-38].

Regarding to the magnetic properties, MAG-8 and MAG-1 showed Ms values of around 40 emu/g. Those resulted lower comparing to bare MAG. The difference could be attributed to the lack of crystallization of the later compared with the first ones (Supplementary material (a)).

3.2- Effect of visible Light

To analyze the impact of the visible light on MNPs properties, the synthesis was performed without irradiation (MAG-6). In this case, 400mg of SDS and NaOH were employed (similarly than MAG-1 formulation). Applying this methodology MAG-6 maintained the same crystalline pattern than raw magnetite, as reveal the XRD data included in Figure 1c.

FTIR spectra of MAG-1 and MAG-6 were compared. In both cases, typical bands of Fe_3O_4 and SDS could be distinguished. No significant differences were observed between both formulations (Supplementary material (b)).

Random shapes around the entire sample was found examining MAG-6 by TEM. Nanorods, spheres and mainly nanocubes were observed. In fact, only slight differences were noted regarding to MAG-1´s morphology (See Figure 3). Hydrodynamic diameters measured in water dispersions revealed that the light plays a role on the size of the particles. An increment of near 100% in the HD of MAG-6 with respect to the corresponding to MAG-1 was registered. (See Table 2).

The ζ of this formulation was maintained negative in sign whereas its magnitude was slightly lower than in the case of MAG-1 (see Table 2).

The application of visible light is not a common practice in iron oxide synthesis, few articles are currently found in open literature in this regard[26,27].The presence of light has an effect of the reaction rate. In the initial stages, in the co-precipitation media $Fe^{2+,}$ Fe^{3+} and SDS are present in aqueous environment. In view of the Lewis acid nature of Fe ions is highly feasible that transfer complex Fe-SDS could be formed[39,40].Such complex absorbs visible light and induce charge transfer between Fe^{2+} ion and the H_2O molecules from the co-precipitation media. As a result, O_2/HO_2 radicals are formed and further oxidize Fe^{2+}/Fe^{3+} ions, leading to an acceleration of the reaction [26]. Consequently, it is possible to obtain a mayor number of nucleus in formation that grows up more quickly. On this way, roughly monodisperse magnetite nanoparticles may be obtained by ending the nucleation process in the initial stages [33], limiting the aggregation trend. Therefore the real impact of the presence of visible light during the MNPs formation is detected in the size and aggregation trend; in agree with recent published works [25].

3.3-Effect of the kind of base and the final reaction volume

MAG was prepared using 400mg of SDS and NH_4OH instead of NaOH as alkali (MAG-9). Under these conditions, no differences were registered between the main properties of MNPs achieved from both procedures.

An additional synthesis was performed using NH_4OH aiming to reach almost the same pH than in the case of NaOH. A greater alkali volume was required in this case. Hence, 100ml of NH_4OH was added dropwise to 100mL of ferric/ferrous precursors. This modification represented an alteration of the final reaction volume, changing from roughly 137 mL (MAG-1) to 200 mL (MAG-4).

Under these conditions, the crystalline analysis by XRD demonstrated that the main product of this reaction was magnetite. Comparing XRD diffractograms of MAG-1 and MAG-4, narrower peaks were found in the corresponding to MAG-4 (see Figure 1c).This data may be associated to the lower size of MAG-1compared with MAG-4(see Table 2). Besides HD data, these differences were evidenced in the sizes estimated by TEM and from Scherrer equation, as it is shown in Table 3. It is worth mention that those sizes also agreed with the ones calculated from magnetic measurements (see Table 3).

The FTIR analysis revealed that the typical band of Fe-O appeared in all the spectra (MAG-9 and MAG-4) as well as slight peaks at 2500-2800 cm^{-1} attributed to CH_2-CH_3 from SDS (Supplementary material (c)).

The variation of the base and final volume did not affect the ζ in a great magnitude (see Table 2). The real differences were appreciated in the morphology and aggregation tends of the MNPs. Figure 4 shows TEM micrographies of MAG-4 and MAG-9. The main difference found when comparing both, MAG-4 and MAG-9, with MAG-1 is that the formers are composed almost exclusively by spherical particles of individual sizes lower than 15nm. Scarce rods formation was observed along both formulations. The trend to aggregation seems to be higher in the case of MAG-9, which may be associated to the low final volume on the synthesis.

The use of NH_4OH instead of NaOH also played an influence in this regard. The evolution of the pH along the reaction procedure in the synthesis of MAG-4 was compared with the trend observed during MAG-1 preparation. It was found that the progress was almost similar (see Figure 5), along the co-precipitation process, with slight variation in the final pH reached after purification. This fact reinforced the idea of the increment of the final volume as responsible for the MAGs properties.

It is worth noting that this condition (final reaction volume) has not been earlier reported as a determinant factor in MNPs shape and size during co-precipitation. Our hypothesis is that this feature retards the interparticle interactions, allowing a more effective stabilization by the SDS molecules. The growth of the particles is also restricted by the rate of precipitation. It is worth mention that each NH_4OH added drop, raises slightly the pH of the mixture, retarding the magnetite formation.

The effect of this experimental variable was also reflected in the magnetic properties of MAGs. In the case of MAG-7 and MAG-4, an irreversibility at temperatures higher than room temperature was evidenced. These data may associate with an average diameter of particle of about 7nm (aprox.;see Table 3). The mentioned data was also used to achieve the M dependence with T under zero field cool (ZFC) and field cool (FC). A maximum near TB=100K was found that represents particles of about 4.5nm aprox. (considering them spherical in shape). Ms values of MAG-4 and MAG-7 were around 80emu/g which are very close to the Ms registered for raw magnetite, suggesting high crystallinity of the particles.

3.4-Effect of the addition order: Inverse co-precipitation.

The synthesis procedure was altered by adding the Fe^{2+}/Fe^{3+} solution (containing 400mg of SDS) dropwise on the alkali (37.20 mL of NaOH 5M) under the influence of light and r.t.

The Figure 1c depicts the XRD diffractograms of MAG-1 and MAG-5, where it is clear that the spinel structure of magnetite was not modified by experimental conditions.

According to the width of the peaks; it is possible assume that the crystalline level of MAG-5 is considerably lower than the corresponding to MAG-1. Even more, signals associated to crystalline planes 111, 422 and 620 are slightly detected in the MAG-5 diffractogram.

From FTIR the presence of both magnetic and SDS moieties was verified (Supplementary material (d)). The surface charge did not vary enough regarding to the data related to MAG-1 and MAG-7 whereas the HD of MAG-5 is comparable to the corresponding to MAG-1(see Table 2). However, the morphology demonstrated to be visibly different. The Figure 6a shows TEM micrographies of MAG-5, where rods of different length may be observed. The nanorods sizes, estimated by TEM images, demonstrated that the formulation was quite heterogeneous. In spite of this, it appeared to be uniform in terms of the shape. This fact represents a great advance when comparing with the earlier described formulations.

Under the conditions of MAG-5 preparation, the reaction rate was greatly increased by the addition of Fe^{2+}/Fe^{3+} solution, containing SDS, on the alkali solution.

In this case, it may infer that increasing precipitating rate greatly influenced surface energy of each crystallographic plane, affecting its growth; and hence determining the preferential growth of certain planes [38].

The magnetic data of MAG-5 are included in Figure 6b in terms of magnetization as a function of applied magnetic field. The magnetization curve of raw magnetite (MAG-7) was also included to compare. Superparamagnetic character was observed in both samples. In the case of MAG-5, its magnetization to saturation diminished in a proportion of about 50%with respect to MAG-7.This reduction may be ascribed to the lower crystallinity of MAG-5 compared with MAG-7.

From the analysis of magnetic data it emerges that the size distribution is narrow and individual particles on the order of 4.5nm could be predicted. This is, apparently, inconsistent with data from TEM images (see Table 3), where nanorods of higher size were observed. From magnetic data, and in accordance with crystallite size obtained from XRD (see Table 3), it may infer that the nanorods are not well crystallized but are mainly composed of a succession of crystallites of around 4.5nm that were not consolidated in a unique monocrystal. [26].

The inverse co-precipitation enabled a rapid formation of very small magnetite crystallites. When a high concentration of these crystallites was formed, they tend to aggregate to form higher size particles without coalescence. This justifies the lack of crystallinity and the sizes obtained by TEM and Scherrer equation (Table 3).

3.5-Stability of MAG formulations

The stability of different formulations was examined though two different criteria on the base of their future applications: i-by the evolution of their sizes (HD) along the time; ii-by their capability to form stable dispersions in different media.

The Figure 7 shows photographs of MAG-8 in organic and aqueous medium. It is evident that in non-aqueous environment, the particles exhibited great aggregation trend and poor dispersion. MAG-8 was taken as example since the same behaviour was observed in all the prepared MNPs. To justify the hydrophilic nature the role of SDS must be considered. When large SDS concentrations were employed (MAG-8), the surfactant molecules interact with magnetic core by means of SO_4^{2-} groups forming a bilayer. This structure rendered MNPs with surface exposed SO_4^{2-}groups (see Scheme 2) [12].

In the case of other MAG formulations where lower nominal SDS concentration was used, some surfactant molecules seem to stabilize by their only presence in aqueous dispersion. This hypothesis is consistent with TG and FTIR data; since not enough evidences of SDS presence was observed analysing TG curves and FTIR obtained from dried MAG-1, MAG-5 and MAG-7 (Supplementary material (e)). To further support this hypothesis a recent work may be considered [22]. In this contribution, the authors attributed the stabilizing effect of PEG on magnetite nanoparticles even when this polymer was not found in the dry particles. They argued that due to its water solubility, PEG´s action is effective only in aqueous dispersions whereas not chemical of physical linkage of surfactant on magnetic core may be detected when water is removed.

Regarding to the evolution of HD as a function of the time; aqueous dispersion of all MAGs were storage and HD was measured after certain periods of time. The data arising from these assays was included in Figure 8; expressed as HD vs. time (days). From the Figure it is possible to infer that all the formulations were stable during at least 30 days. That means that the stabilization mechanism imparted by the surfactant and by the preparation conditions is of long term ensuring MNPs able to conserve their initial size along the time. Only selected formulations exhibited slight variations on their HD during longer periods.

5. CONCLUDING REMARKS

This work provides insight on the controlled synthesis of magnetite nanoparticles using the simple co-precipitation method. Notable differences regarding to the traditional procedure were implemented. Mild conditions, including room temperature and absence of inert atmosphere, were using. Further, the novel application of visible light was adopted along the process. Under these conditions, magnetite was almost exclusively obtained.

We demonstrated that MNPs with specific shape and size may be obtained by the proper modification of experimental variables. The surfactant, in this case SDS, was a determining factor of the particles shape as well as on the dispersability properties of magnetic nanosystems.

The rate of precipitation influenced the shape favouring the formation of MNPs of about 4.5nm oriented in sequence, defining nanorods of higher sizes.

The kind of base appeared not to have a great effect on MNPs properties, under the explored conditions, while the final reaction volume resulted crucial.

Highly stable hydrophilic formulations were obtained within this methodology. The reached characteristics on MNPs are of great importance in terms of their potential applications in biomedical field. The most interesting task is related to the simplification of the traditional preparative methodology and the wide gamma of shapes and sizes that are possible to attain.

6. ACKNOWLEDGEMENTS

The authors acknowledge the financial support of CONICET, and UNS (PGI24/ZQ09).

7. REFERENCES.

[1] J.Y. Huang, M.H Chen, W.T. Kuo, Y.J. Sun, F.H. Lin. The characterization and evaluation of cisplatin-loaded magnetite–hydroxyapatite nanoparticles (mHAp/CDDP) as dual treatment of hyperthermia and chemotherapy for lung cancer therapy. Ceram. Int.41 (2015) 2399-2410.

[2]J.D. Obayemi, S. Dozie-Nwachukwu, Y. Danyuo, O.S. Odusanya, N. Anuku, K. Malatesta, W.O. Soboyejo. Biosynthesis and the conjugation of magnetite nanoparticles with luteinizing hormone releasing hormone (LHRH). .Mate. Sci. Eng., C.46 (2015) 482-496.

[3]S. Laurent, D.Forge, M.Port, A.Roch, C. Robic, L. Vander Elst, RN. Muller. Magnetic iron oxide nanoparticles: synthesis, stabilization, vectorization, physicochemical characterizations, and biological applications. Chem. Rev.108 (2008) 2064-2110.

[4] A. Rodríguez-López, J.J. Cruz-Rivera, C.G. Elías-Alfaro, I. Betancourt, H. Ruiz-Silva, R. Antaño-LópezFine tuning of magnetite nanoparticle size distribution using dissymmetric potential pulses in the presence of biocompatible surfactants and the electrochemical characterization of the nanoparticles. Mate. .Sci. Eng., C.46 (2015) 538-547A.

[5] K. Chatterjee, S. Sarkar, K. Jagajjanani Rao, S. Paria. Core/shell nanoparticles in biomedical applications. Adv. Colloid Interfac.209 (2014) 8-39 K.

[6] D.D. Herea, H. Chiriac, N. Lupu, M. Grigoras, G. Stoian, B.A. Stoica, T. Petreus. Study on iron oxide nanoparticles coated with glucose-derived polymers for biomedical applications. Appl. Surf. Sci.352(2015) 117–125

[7]N. Lupu, Source: Nanowires Science and Technology, ISBN 978-953-7619-89-3, pp. 402, INTECH, Croatia, 2010

[8] S. Khoee, H. Shagholani, N. Abedini. Synthesis of quasi-spherical and square shaped oligoamino-ester graft-from magnetite nanoparticles: Effect of morphology and chemical structure on protein interactions. Polymer 56 (2015) 207-217.

[9] M.P. Calatayuda, B. Sanz, V. Raffa, C. Riggioc, M.R. Ibarra, G.F. Goya. The effect of surface charge of functionalized Fe_3O_4 nanoparticles on protein adsorption and cell uptake, Biomaterials 35 (2014) 6389-6399.

[10] V. L. Lassalle, M. Avena, M. L. Ferreira. A review of the methods of magnetic nanocomposites synthesis and their applications as drug delivery systems and immobilization supports for lipases. Trends Polym Sci.13 (2009) 37-67.

[11] A. Šutka, S. Lagzdina, T. Käämbre, R. Pärna, V. Kisand, J. Kleperis, M. Maiorov,A. Kikas, I. Kuusik, D. Jakovlevs. Study of the structural phase transformation of iron oxide nanoparticles from an Fe^{2+} ion source by precipitation under various synthesis parameters and temperatures. Mater. Chem. Phys.149-150 (2015) 473-479.

[12] H. Li, L.Qin, Y. Feng, L. Hu, C. Zhou. Preparation and characterization of highly water-soluble magnetic Fe_3O_4 nanoparticles via surface double-layered self-assembly method of sodium alpha-olefin sulfonate. J. Magn Magn Mater. 384 (2015) 213–218.

[13] S. Rani, G.D.Varma. Superparamagnetism and metamagnetic transition in Fe_3O_4nano-particles synthesized via co-precipitation method at different pH. Physica B. 472(2015) 66–77.

[14] M. L. Mojica Pisciotti, E. Lima Jr., M. Vasquez Mansilla, V. E. Tognoli, H. E. Troiani, A. A. Pasa, T. B. Creczynski-Pasa, A. H. Silva, P. Gurman, L. Colombo, G. F. Goya, A. Lamagna and R. D. Zysler. In vitro and in vivo experiments with iron oxide nanoparticles functionalized with dextran or polyethylene glycol for medical applications: Magnetic targeting. J Biomed Mater Res-A. 102 (2014) 860–868.

[15] P. Nicolas, M. Saleta, H. Troiani, R. Zysler, V. Lassalle, M. L. Ferreira. Preparation of iron oxide nanoparticles stabilized with biomolecules: Experimental and mechanistic issues, Acta Biomater.9 (2013) 4754–4762.

[16]M. A. Agotegaray, S. Palma, V. Lassalle. Novel chitosan coated magnetic nanocarriers for the targeted Diclofenac delivery. J Nanosci Nanotechnol.14 (2014) 3343-3347.

[17]M. A. Agotegaray, V. Lassalle. Study of the Experimental Conditions and Mechanisms for Diclofenac Loading in Functionalized Magnetic Nanoparticles. IJCPA.1(2014)154-164

[18] H.C. Roth, S.P. Schwaminger, M. Schindler, F.E. Wagner, S. Berensmeier. Influencing factors in the co-precipitation process of superparamagnetic iron oxide nanoparticles: A model based study. J. Magn. Magn. Mater.377 (2015) 81–89.

[19] M. Fang, V. Strom, R.T Olsson, L. Belovaand, K V Rao. Particle size and magnetic properties dependence on growth temperature for rapid mixed coprecipitated magnetite nanoparticles. Nanotechnology 23 (2012) 145601 (9pp)

[20] M.C. Mascolo, Y. Pei, T.A. Ring. Room Temperature Co-Precipitation Synthesis of Magnetite Nanoparticles in a Large pH Window with Different Bases. Materials.6 (2013) 5549-5567.

[21] M. Adeli, Y.Yaminib, M. Faraji. Removal of copper, nickel and zinc by sodium dodecyl sulphate coated magnetite nanoparticles from water and waste water samples. Arab J. Chem. In press.doi:10.1016/j.arabjc.2012.10.012 (2012).

[22] M. Sun, A. Zhun, Q. Zhang, Q. Liu. A facile strategy to synthesize monodisperse superparamagnetic OA-modified Fe_3O_4 nanoparticles with PEG assistant. J. Magn. Magn. Mater.369 (2014) 49–54.

[23] I. Nedkova, T. Merodiiskaa , L. Slavova , R.E. Vandenbergheb , Y. Kusanoc , J. Takada. Surface oxidation, size and shape of nano-sized magnetite obtained by co-precipitation. J. Magn. Magn. Mater.300 (2006) 358–367.

[24] W. Zhang, S. Jia, Q. Wu, J. Ran, S. Wu, Y. Liu. Convenient synthesis of anisotropic Fe_3O_4nanorods by reverse co-precipitation method with magnetic field-assisted. Mater. Lett.65 (2011) 1973–1975.

[25] Y. Lin, Y. Wei, Y. Sun, J. Wang. Synthesis and magnetic characterization of magnetite obtained by monowavelength visible light irradiation. Mater. Res. Bull. 47. (2012) 614–618.

[26] Z. Chen, Z. Geng, T. Tao, Z. Wang. Shape-controlled synthesis of Fe_3O_4 rhombic dodecahedrons and nanodiscs. Mater. Lett.117 (2014)10–13.

[27] S.Lazhen, Q.Yongsheng, G.Yong, M.Shuangming, Y.Guochen, W.Meixia,Z.Jianguo. Facile co-precipitation synthesis of shape-controlled magnetite nanoparticles. Ceram Int. 40 (2014) 1519–1524.

[28]V. Lassalle, R. Zysler, M. L. Ferreira. Novel and facile synthesis of magnetic composites by a modified co-precipitation method. Mater. Chem. Phys. 130 (2011) 624-634.

[29]S.L. Tie, Y.Q. Lin, H.C. Lee, Y.S. Bae, C.H. Lee. Amino acid-coated nano-sized magnetite particles prepared by two-step transformation. Colloids Surface. A. 273 (2006) 75–83.

[30]D-Lee, K. M. Ponvel, M. Kim, S. Hwang, I-S. Ahn, C-H. Lee. Immobilization of lipase on hydrophobic nano-sized magnetite particles. J. Mol. Catal. B- Enzym. 57 (2009) 62–66.

[31]Joint Committee on Powder Diffraction Standards. Anal. Chem. 42 (1970) pp 81A–81A. doi**:**10.1021/ac60293a779.

[32] A. Sutka , S. Lagzdina , T. Kaambre , R. Parna , V. Kisand , J. Kleperis, M. Maiorov ,A. Kikas, I. Kuusik , D. Jakovlevs. Study of the structural phase transformation of iron oxide nanoparticles from an Fe^{2+} ion source by precipitation under various synthesis parameters and temperatures, Mat. Chem. and Phys. 149-150 (2015) pp 473-479.

[33]. L. Zhang, R. He, H-C.Gu. Synthesis and kinetic shape and size evolution of magnetite nanoaprticles. Mater. Res. Bull. 41 (2006) 260–267

[34]J. Cheon, N-J. Kang, S-M. Lee, J-H Lee, J-H Yoon, S. J. Oh. Shape Evolution of Single Crystalline Iron Oxide Nanocrystals. J. Am. Chem. Soc. 126 (2004) 1950–1951.

[35] M.V. Kovalenko, M.I. Bodnarchuk, R.T. Lechner. Fatty acid salts as stabilizers in size- and shape-controlled nanocrystal synthesis: the case of inverse spinel iron oxide. J. Am. Chem. Soc. 129 (2007)6352–6353.

[36] Z.L. Wang, Handbook of Nanophase and Nanostructured Materials— Vol. II: Characterization, firts ed., Springer US, 2002.

[37] V.F. Puntes, D. Zanchet, C.K. Erdonmez, A.P. Alivisatos. Synthesis of hcp-Co Nanodisks. J. Am. Chem. Soc.124 (2002) 12874-12880.

[38] T. Ahn, J. H. Kim, H-M. Yang, J.W. Lee, J-D. Kim. Formation Pathways of Magnetite Nanoparticles by Coprecipitation Method. J. Phys. Chem. C.116 (2012) 6069−6076.

[39] E .Pramauro , E. Pelizzetti , S. Diekmann , J. Frahm. Electron transfer in micellar systems.Separation of electrostatic and environmental effects for some electron-transfer reactions in micellar solutions of sodium dodecyl sulphate. Inorg. Chem. 21 (1982) 2432-2436

[40] J-Y. Park, J.-H. Kim. Role of sol with iron oxyhydroxide/sodium dodecyl sulfate composites on Fenton oxidation of sorbedphenanthrene in sand. J. Environ. Manage. 126 (2013) 72-78**.**

Figures Captions

Fig 1: (a) FTIR spectra of MAG-7, MAG-1 and MAG-8.

(b). FTIR spectrum of SDS. (c). XRD diffractograms of MAG-1, MAG-4, MAG-5, MAG-6 and MAG-7.

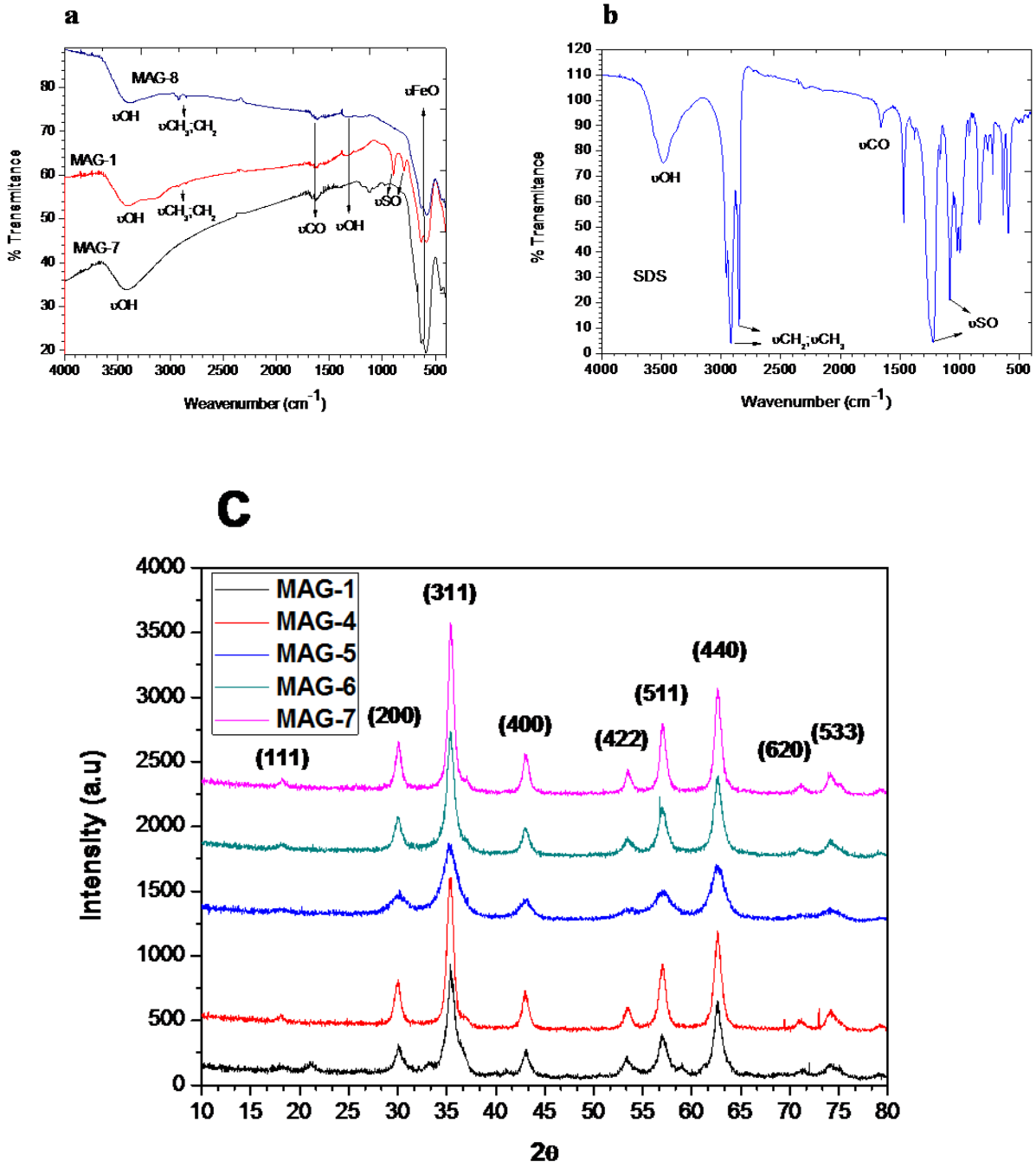

Fig 2: (a). TEM images and DLS plot of MAG-7. (b). TEM images and DLS plot of MAG-1. (c). TEM images and DLS plot of MAG-8.

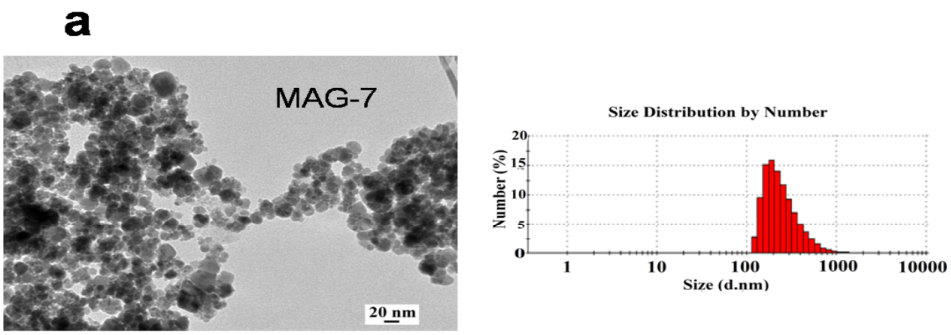

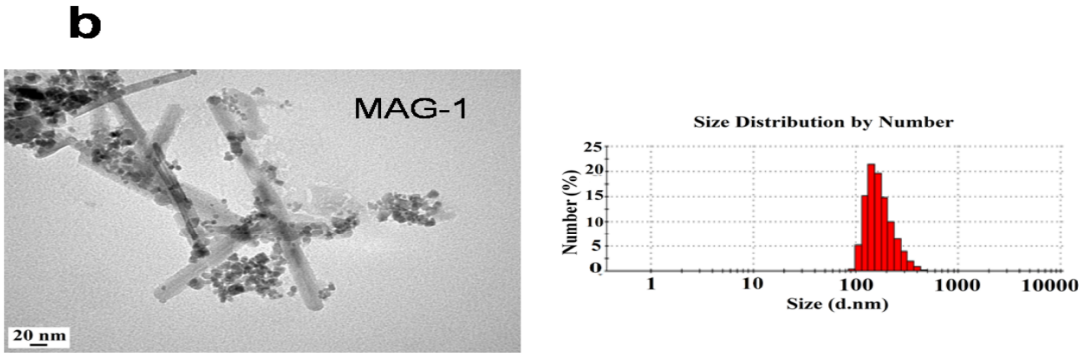

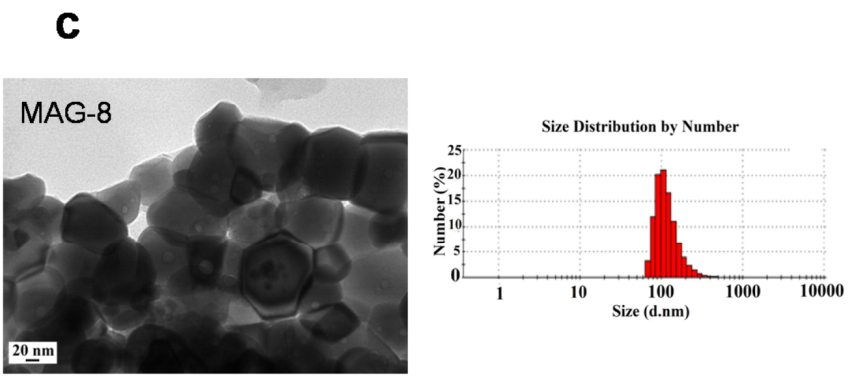

Fig 3: TEM images of MAG-1 and MAG-6.

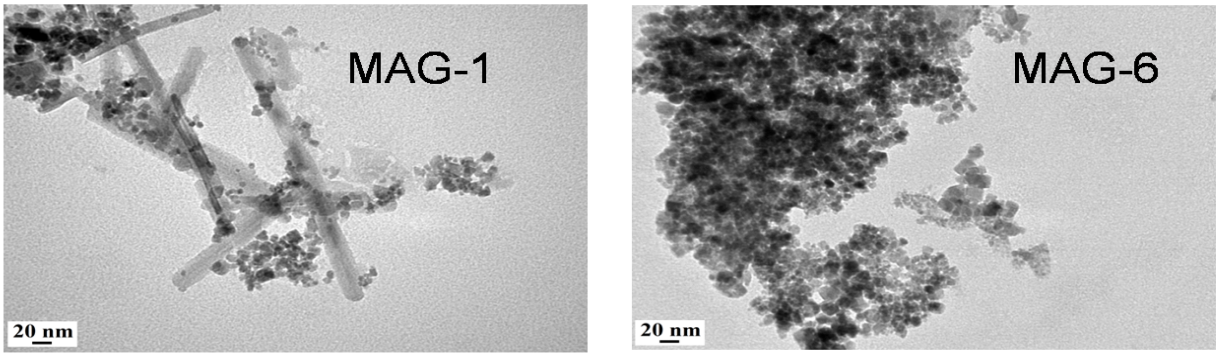

Fig 4: TEM images of MAG-4 and MAG-9.

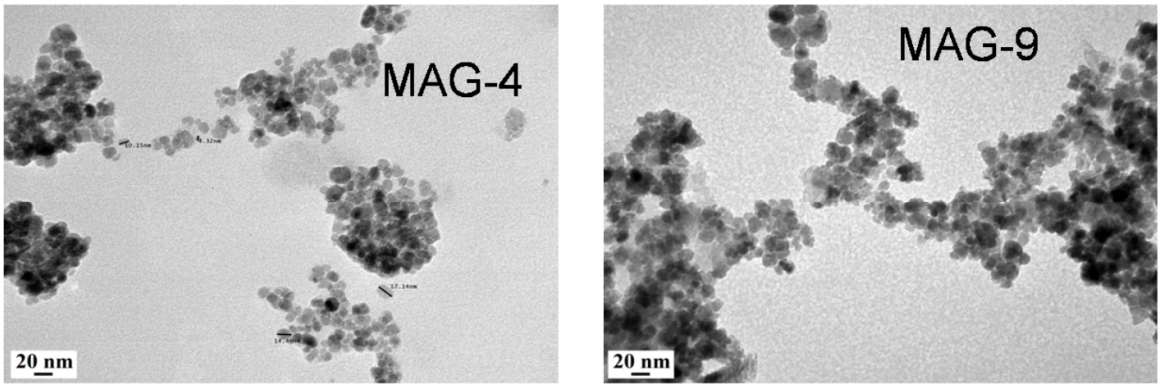

Fig. 5: pH evolution during the progress of co-precipitation reaction.

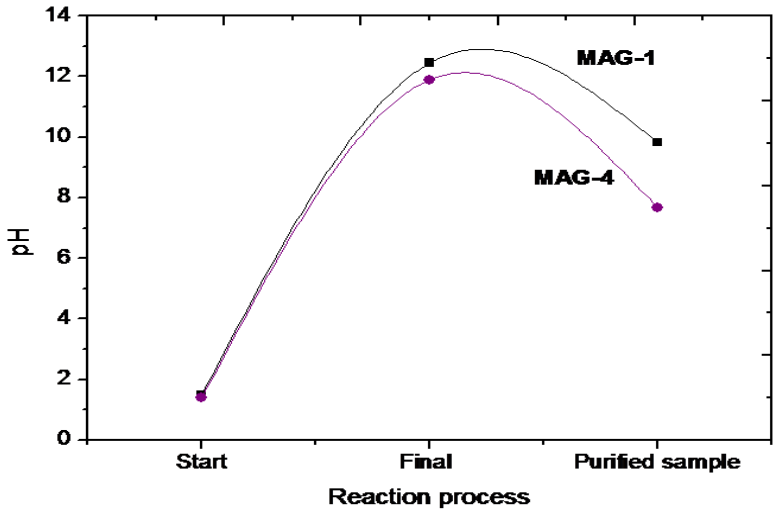

Fig. 6. (a). TEM image of MAG-5. **(**b) Magnetic properties of MAG-5 and MAG-7.

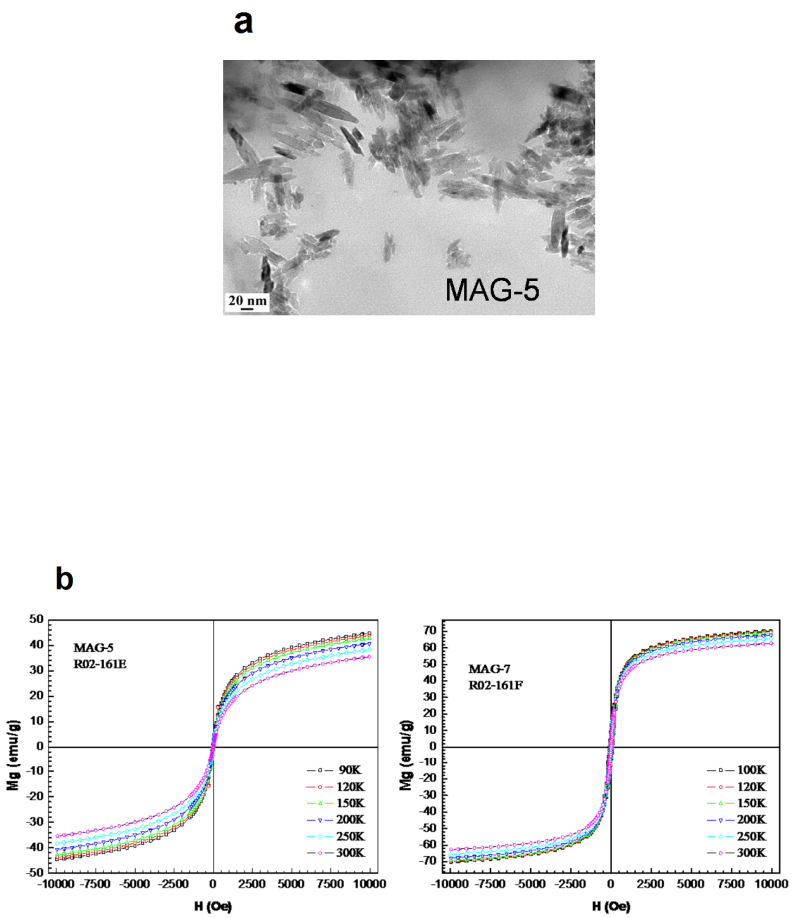

Fig. 7: Photographs of MNPs dispersions in: a-water; b-ethanol/water, c-acetone.

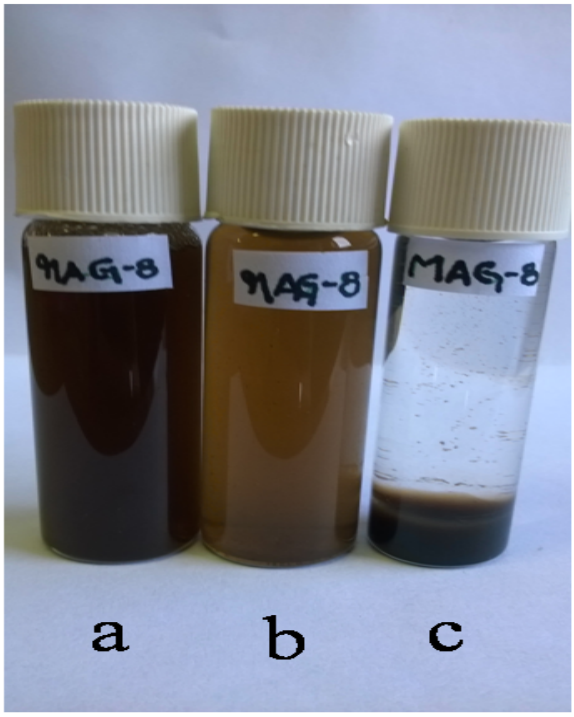

Fig. 8: Evolution of the HD as a function of the time.

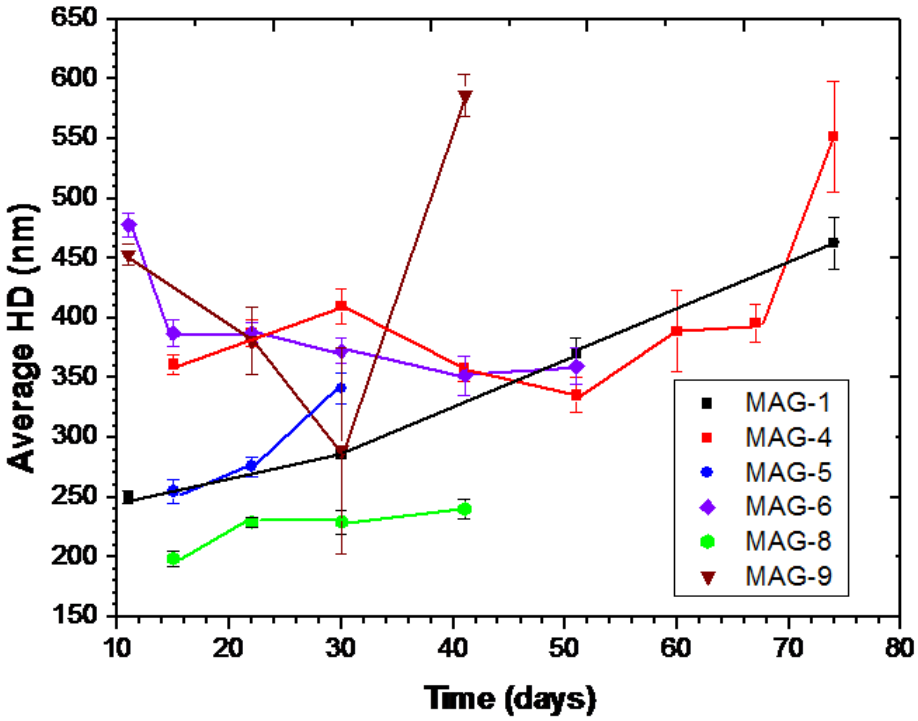

Scheme 1. Co-precipitation method. (a) Traditional synthesis. (b) Inverted synthesis.

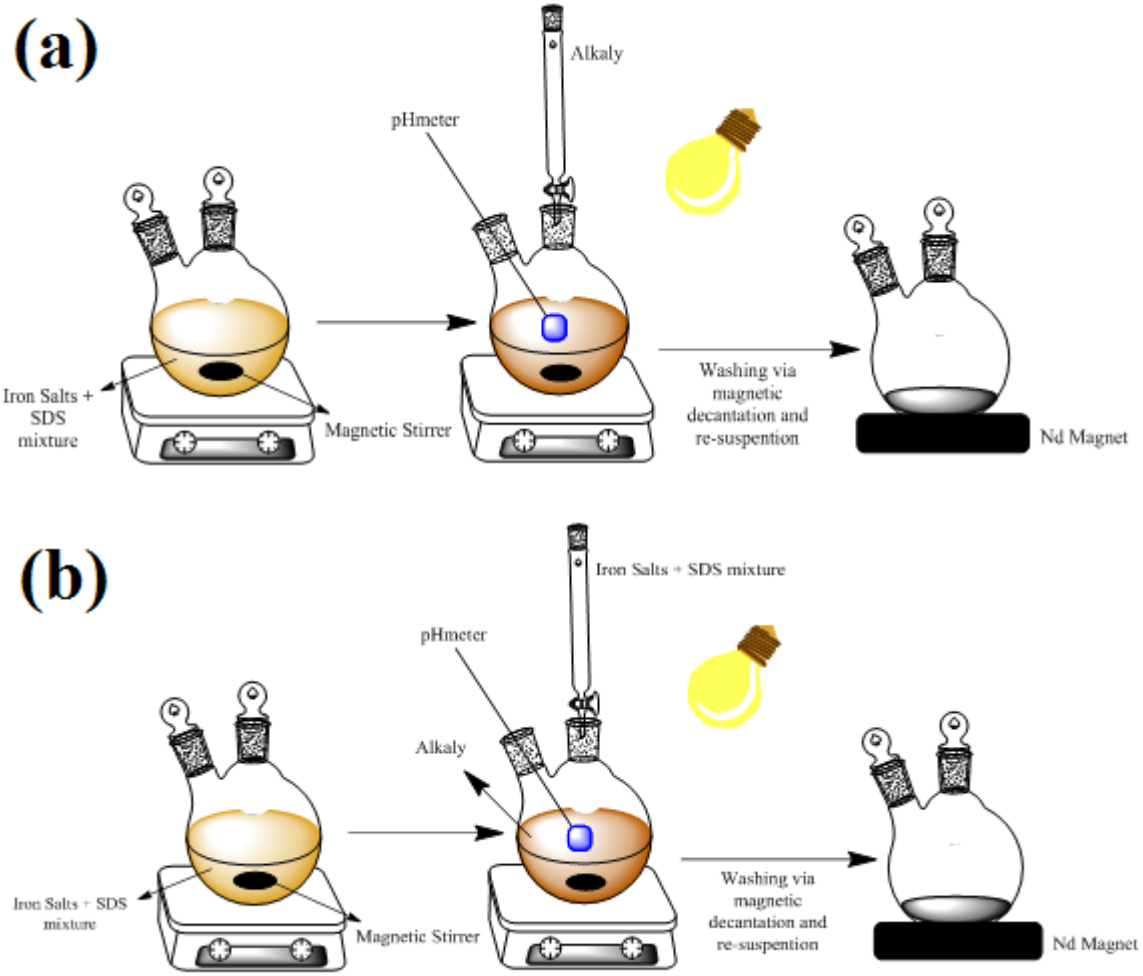

Tables Captions

Table 1. Experimental conditions explored in each MAG formulation.

Sample	*Moles of SDS*	*Alkali*[1]	*mL of alkali addition*	*Speed of addition (mL/min)*	*Order of addition*	*Molar ratioAlkali/Fe^{2+}+Fe^{3+}*	*Final volume (mL)*	*Light*
MAG-1	< 0.00127	NaOH	37.20	4.13	Alkali to iron precursor solution	6.20	137.20	Yes
MAG-4	0.00127	NH_4OH	100.00	3.33	Alkali to iron precursor solution	16.70	200.00	Yes
MAG-5	0.00127	NaOH	37.25	2.08	Solution of iron precursor to alkali	6.20	137.20	Yes
MAG-6	0.00127	NaOH	17.20	2.90	Alkali to iron precursor solution	2.90	117.20	NO
MAG-7	0.00000	NaOH	16.60	2.80	Alkali to iron precursor solution	2.80	116.60	Yes
MAG-8	0.00346	NaOH	18.30	3.00	Alkali to iron precursor solution	3.05	118.30	Yes
MAG-9	0.00127	NH_4OH	23.00	2.50	Alkali to iron precursor solution	3.83	123.00	Yes

[1.] Alkali concentration: 5M

Table 2. Z-potential (ζ ;mV) and hydrodynamic diameter (HD; nm) of all formulations prepared within this work.

Sample	***Moles of SDS***	***HD (nm)***	***ζ (mV) pH: 6.8-7.0***
MAG-1	< 0.00127	249.9 ± 5.74 *PDI:* 0.350 ± 4.80x10^{-3}	-30.6 ± 2.80
MAG-4	0.00127	361.3 ± 8.00 *PDI:* 0.391 ± 1.70x10^{-3}	-33.1 ± 0.61
MAG-5[1*]	0.00127	254.6 ± 9.80 *PDI:* 0.245± 3x10^{-2}	-35.5 ± 3.70
MAG-6	0.00127	477.9 ± 9.70 *PDI:* 0.290 ± 3.80x10^{-2}	-26.4 ± 0.51
MAG-7	0.00000	401 ± 5.46 *PDI*: 0.264 ± 1.90x10^{-2}	-34.2 ± 0.51
MAG-8	0.00346	198.5 ± 6.41 *PDI:* 0.199 ± 1.20x10-2	-32.1 ± 1.60
MAG-9	0.00127	453.2 ± 8.62 *PDI:* 0.202 ± 3x10^{-2}	-34.5 ± 0.11

*[1] Ethanol/Water media= 50:50

The data is an average of roughly 5-7 measurements.

Table 3.Estimation of nanoparticles sizes based on TEM and Scherrer Equation data.

Sample	***Size estimated by TEM (nm)***	***Size estimated by XDR(nm)***
MAG-1	Nanorods 193.37 ± 14.84 x 14.89 ± 5.53	8.22
MAG-4	11.51± 5.60 [a]	11.77
MAG-5	Nanorods 35.3 ± 6.50 x 5.60 ± 1.55 [b]	6.09
MAG-6	10.00 ± 3.62	12.45
MAG-7	16.30 ± 7.50 [c]	13.83

[a]Size estimated by magnetic properties: higher than 7nm

[b]Size estimated by magnetic properties: 4.5nm

[c]Size estimated by magnetic properties: higher than 7nm